10-2011

Cdc42 Regulates Extracellular Matrix Remodeling in Three Dimensions*

Nisha S. Sipes
University of Cincinnati

Benjamin Feng
Grand Valley State University, fengb@gvsu.edu

Fukun Guo
University of Cincinnati

Hyung-Ok Lee
Fox Chase Cancer Center

Fu-Sheng Chou
University of Cincinnati

See next page for additional authors

THE JOURNAL OF BIOLOGICAL CHEMISTRY VOL. 286, NO. 42, pp. 36469–36477, October 21, 2011

Cdc42 Regulates Extracellular Matrix Remodeling in Three Dimensions*[S]

Received for publication, July 15, 2011, and in revised form, August 8, 2011 Published, JBC Papers in Press, August 31, 2011, DOI 10.1074/jbc.M111.283176

Nisha S. Sipes[‡§], Yuxin Feng[‡], Fukun Guo[‡], Hyung-Ok Lee[¶], Fu-Sheng Chou[‡§], Jonathan Cheng[¶], James Mulloy[‡§], and Yi Zheng[‡§1]

From the [‡]Division of Experimental Hematology and Cancer Biology, Children's Hospital Medical Center and [§]Department of Cell and Cancer Biology, University of Cincinnati, Cincinnati, Ohio 45229 and the [¶]Department of Medical Oncology, Fox Chase Cancer Center, Philadelphia, Pennsylvania 19111

Extracellular matrix (ECM) actively participates in normal cell regulation and in the process of tumor progression. The Rho GTPase Cdc42 has been shown to regulate cell-ECM interaction in conventional two-dimensional culture conditions by using dominant mutants of Cdc42 in immortalized cell lines that may introduce nonspecific effects. Here, we employ three-dimensional culture systems for conditional gene targeted primary mouse embryonic fibroblasts that better simulate the reciprocal and adaptive interactions between cells and surrounding matrix to define the role of Cdc42 signaling pathways in ECM organization. Cdc42 deficiency leads to a defect in global cell-matrix interactions reflected by a decrease in collagen gel contraction. The defect is associated with an altered cell-matrix interaction that is evident by morphologic changes and reduced focal adhesion complex formation. The matrix defect is also associated with a reduction in synthesis and activation of matrix metalloproteinase 9 (MMP9) and altered fibronectin deposition patterning. A Cdc42 mutant rescue experiment found that downstream of Cdc42, p21-activated kinase (PAK), but not Par6 or WASP, may be involved in regulating collagen gel contraction and fibronectin organization. Thus, in addition to the previously implicated roles in intracellular regulation of actin organization, proliferation, and vesicle trafficking, Cdc42 is essential in ECM remodeling in three dimensions.

The extracellular matrix (ECM)[2] participates in tissue development, tissue homeostasis, wound healing, and tumor metastasis (1). Fibroblasts seeded into a three-dimensional collagen matrix have been a model system for studying this interaction between cell and ECM (2–5). The three-dimensional culture environment more closely mimics the natural *in vivo* environment with the cell surrounded by ECM rather than on a non-physiological two-dimensional culture dish surface, which is also reflected by unique signaling events of cells in three-dimensional *versus* two-dimensional culturing (4, 6, 7).

Fibroblasts grown in a floating three-dimensional collagen matrix deposit and remodel the surrounding ECM through mechanical interactions between the cells and the ECM and through secreted proteases (2, 8). Contraction of the matrix is a visible readout of cell-matrix interactions that are indicative of changes in ECM reorganization. First, as in wound healing, fibroblasts exert mechanical force on the surrounding ECM, leading to matrix contraction (9, 10). Focal complexes, which form a mechanical link between ECM and the cytoskeleton of the cell and can initiate intracellular signaling cascades, are critically involved in this process (11, 12). Second, matrix metalloproteinases (MMPs) and/or other proteases produced by fibroblasts can degrade the surrounding ECM and have been shown to play a role in matrix contraction (8, 13, 14). Although the mechanisms remain unclear, MMPs may regulate contraction through ECM cleavage and degradation, interfering with tractional forces and migration, and/or competing with cell matrix adhesion proteins (8, 13, 14).

The Rho GTPases Rac1, RhoA, and Cdc42 are known to regulate intracellular activities such as focal complex formation, integrin localization, adhesion, cell morphology, and cytoskeletal organization, as well as MMP expression and activation, activities that are important for ECM contraction (15–19). Most previous studies have been performed under traditional two-dimensional culture conditions, although the roles of Rac1 and RhoA have been examined in regulating three-dimensional ECM remodeling to some extent (17, 20, 21). Furthermore, most studies employed broad ranged activators, inhibitors, and/or dominant mutants of Rho GTPases, which are inherently limited by their nonspecific nature toward individual Rho GTPases involved in the cellular process (22, 23). In particular, the potential role of Cdc42 in ECM remodeling has not been reported in three-dimensional systems.

The goal of our studies is to define the signaling role of Cdc42 in three-dimensional ECM remodeling. We have utilized a collagen three-dimensional culture system and Cdc42 conditional gene deletion in primary mouse embryonic fibroblasts (MEFs) that simulate the reciprocal and adaptive interactions between cells and surrounding matrix. We report that Cdc42 is a key regulator of cell-ECM interactions, specifically in maintaining normal cell morphology, focal complex formation, MMP9 expression and activation, and extracellular fibronectin organization. The inside-out effect by Cdc42 on collagen contraction

* This work was supported, in whole or in part, by National Institutes of Health Training Grant T32 HD046387 (to N. S. S.) and by National Institutes of Health Grants R01 CA150547 and R01 HL085362 (to Y. Z.). This work was also supported by the Robert and Emma Lou Cardell Fellowship (to N. S. S.).

[S] The on-line version of this article (available at http://www.jbc.org) contains supplemental Figs. 1–8.

[1] To whom correspondence should be addressed: Div. of Experimental Hematology and Cancer Biology, Children's Hospital Medical Center, 333 Burnet Ave., Cincinnati, OH 45229. Tel.: 513-636-0595; Fax: 513-636-3768; E-mail: yi.zheng@cchmc.org.

[2] The abbreviations used are: ECM, extracellular matrix; MMP9, matrix metalloproteinase 9; PAK, p21-activated kinase; FAK, focal adhesion kinase.

and fibronectin matrix organization is associated with the effector PAK. Our findings implicate Cdc42 as an important regulator of ECM organization in three dimensions.

EXPERIMENTAL PROCEDURES

Generation of Primary Cdc42$^{loxP/loxP}$ MEFs—The generation and genotyping of Cdc42 conditional knock-out mice was described previously (24). MEFs were generated from mouse embryos at gestational ages E12–13. MEFs were cultured in DMEM (Invitrogen) and supplemented with 10% heat-inactivated FBS as described previously (25). These cells were used at low passage numbers (<5) to avoid accumulation of genetic abnormalities.

Adenoviral Deletion—Deletion of Cdc42 from Cdc42$^{loxP/loxP}$ MEFs was achieved by infecting twice with 25 multiplicity of infection adenoviral Cre recombinase a day apart. The experiments were initiated at 4 days after infection to ensure efficient Cdc42 protein deletion. Wild-type MEFs were also infected as positive controls.

Collagen Gel Contraction Assay—For collagen gel contraction, MEFs were trypsinized, suspended in cold normal medium, counted, and suspended at 50,000, 100,000, or 150,000 cells/60 μl of collagen I solution. Collagen I solution consisted of 46.5% normal media, 2% $NaHCO_3$, 1.5% 1 M Hepes, 50% PurCol (3.0 mg/ml, Inamed Biomaterials) The 60-μl collagen I solution mixed with cells was placed as a droplet in the center of a six-well sterile non-tissue culture-treated dish and incubated at 37 °C for 20 min to solidify the gel. 2 ml of normal MEF media was added to each well, and the collagen I gel/cell solution was lifted off the bottom with a cell lifter. The initial reading (time point 0) was taken at this step, and the dish was put back into the incubator until further time point readings. Images were taken on an optical microscope (Leica S8AP0; Leica DFC320; LAS; Leica Microsystems, Inc.), and NIH ImageJ software was used to calculate the surface area. Percent contraction was calculated as the change in surface area from the initial surface area divided by the initial surface area. Cell extensions were measured from the cell surface to the tips of the extensions by using confocal images and ImageJ for all cells within a given field (20× objective) in three representative images.

Three-dimensional Fibronectin Assembly Assay—Coverslips were pretreated and cells were plated as described previously (26). Briefly, coverslips were coated with 0.2% gelatin solution, and MEFs were plated at 120,000 cells/15-mm circular coverslip. Ascorbic acid (50 μg/ml) was added to the medium every other day to encourage matrix deposition. Cells were fixed at 2, 4, 6, 8, and/or 9 days post-plating. Fibronectin, F-actin, and nuclei were stained, and the cells and matrix were imaged, as described above. Matrix thickness was assessed using the *z*-stack feature from the confocal by measuring the maximum matrix thickness across a stack of images from five independent sets of cells.

Western Blotting and Immunofluorescence—For Western blotting, MEFs in three-dimensional collagen I after 6 h of plating were lysed in lysis buffer containing 20 mM Tris-HCl (pH 7.6), 100 mM NaCl, 10 mM MgCl, 1% Triton X-100, 0.2% sodium deoxycholate, 2 mM PMSF, 0.5 mM DTT, 50 mM NaF, 1 mM Na_3VO_4, 0.1 μM okadaic acid, 0.1% SDS, and protease inhibitors (Sigma), and protein extracts of 50 μg were used for analysis. For immunoprecipitation, cells were incubated in a buffer containing 50 mM Hepes, pH 7.3, 150 mM NaCl, 1% Triton X-100, 5 mM $MgCl_2$, 1 mM EDTA, 1 mM Na_3VO_4, 10 mM NaF, 10% glycerol, and protease inhibitors (2 mM phenylmethylsulfonyl fluoride, 20 μg/ml leupeptin, 100 μg/ml aprotinin) for 15 min at 4 °C. Extracts were clarified by centrifugation at 14,000 rpm for 15 min. 1 μl of the PAK antibody was incubated with each lysate for 1 h at 4 °C, and then 30 μl of suspended protein A/G-agarose beads (Santa Cruz Biotechnology) were incubated with each lysate for 2 h at 4 °C, all performed while rotating. Beads were pelleted, washed, and lysed. Proteins were resolved by electrophoresis in a 4–15% gradient gel and electrotransferred to a PVDF membrane. Primary antibodies used were anti-cofilin, anti-pcofilin (Ser-3), anti-PAK, anti-pPAK1 (Thr-423)/PAK2 (Thr-402), anti-ERK, anti-pERK1/2 (Thr-202/Tyr-204), anti-MLC, anti-pMLC (Ser-19), anti-paxillin (Tyr-118) (Cell Signaling Technology), anti-Cdc42, anti-focal adhesion kinase, anti-pfocal adhesion kinase (phospho-Tyr-397), anti-paxillin (BD Transduction Laboratories), anti-β-actin, anti-fibronectin (Sigma), anti-pWASP (Ser-483/Ser-484) (Bethyl Laboratories), anti-WASP (Santa Cruz Biotechnology), and GAPDH (Fitzgerald Industries). Secondary antibodies used were horseradish peroxidase-linked anti-mouse or anti-rabbit IgG (Amersham Biosciences). Representative images are shown.

For immunofluorescence experiments, MEFs were plated in collagen I gel (three-dimensional, 20,000 cells/collagen gel), or allowed to produce their own matrix (three-dimensional fibronectin matrix assembly). In addition 50,000 MEFs were plated on collagen-coated glass coverslips (two-dimensional), with collagen coating performed with 80 μg/ml of PurCol in PBS at 37 °C for 2 h on glass coverslips. The three-dimensional and two-dimensional cells were fixed with 3.7% formaldehyde, quenched with NH_4Cl, and permeabilized with 0.1% Triton X-100. The MEFs were blocked with 2% BSA and stained with rhodamine-phalloidin (Molecular Probes), phospho-paxillin (Cell Signaling Technology), TO-PRO-3 (Invitrogen), DAPI (Invitrogen), α tubulin, β tubulin, vinculin, and fibronectin (Sigma). Alexa Fluor 488 (Invitrogen) was used as secondary antibodies for α and β tubulin, and Cy5 (Jackson ImmunoResearch Laboratories) for vinculin and phospho-paxillin. A laser confocal microscope (Zeiss LSM 510) was used to image MEFs and capture optical slices from three-dimensional samples, and the LSM Image Browser (Carl Zeiss MicroImaging GmbH) was used to view the images.

Flow Cytometry—MEFs were prepared in cell dissociation buffer for 10 min at room temperature, washed with PBS, and suspended in 1% fetal bovine serum/PBS. Antibodies (0.5 μl) were added to 250,000 MEFs at room temperature for 20 min and subjected to FACS analysis using Canto III (BD Biosciences). Data were analyzed with FACS Diva software. Antibodies PE-CD49d (integrin α4), PE-CD49e (α5), PE-CD61 (β3), APC-CD11b (αM), and FITC-CD29 (β1) was from BD Biosciences, and PE-CD11a (αL) was from eBiosciences.

Reflection Microscopy—MEFs in three dimensions were prepared as per the immunofluorescence protocol and imaged

using the Zeiss LSM 510 (Zeiss). three-dimensional samples were stained for F-actin (rhodamine-phalloidin) only and imaged for fluorescence (F-actin) and reflected light (collagen fibrils). The HeNe laser (633 nm) was used for reflected light.

Gelatinase Activity Assay—Cells (20,000) were plated in three dimensions with the addition of 0.33 μl of DQ^{TM} gelatin (Molecular Probes) per 60 μl gel. After 6 h, cells were fixed, stained with rhodamine-phalloidin, and imaged. Quantification of protease activity was evaluated on NIH ImageJ. Values were obtained by converting the fluorescent images to 8-bit and summing the intensity values over 90–255 pixel intensity values (any value below 90 pixel intensity value was considered to be background) and dividing by the number of nuclei. On average, 90 nuclei were in each sample. Values were averaged over three experiments, and the S.D. were derived.

Zymography—The culture medium (30 μl) after 6 h of cell plating from the contraction experiment was applied to a 10% Tris-HCl Bio-Rad Ready Gel containing 10% gelatin. Gels were incubated in 2.5% Triton X-100 for 1 h and then incubated for additional 18 h at 37 °C in 50 mM Hepes (pH 7.5), 200 mM NaCl, 5 mM $CaCl_2$, and 20 μM $ZnCl_2$. The gels were then stained with Coomassie Blue.

Quantitative Real-time RT-PCR—Three-dimensional cells (250,000 cells/60 μl gel) were pelleted for protease expression profiling, and cells from the fibronectin matrix assembly were gathered for fibronectin and collagen I expression profiling. mRNA was harvested using an RNeasy Micro Kit (Qiagen). Synthesis of cDNA was carried out using 1 μg of RNA using the High Capacity cDNA Reverse Transcription (Applied Biosystems Inc.). The cDNA for MMP9, collagen I, and fibronectin was amplified using SYBR Green PCR Master Mix reagent (Applied Biosystems) for MMP9, collagen I, fibronectin, and GAPDH. Quantitative real-time RT-PCR was performed and analyzed on an ABI Prism 7500 sequence detection system (Applied Biosystems). Relative expression was calculated using the standard curve. The following primer sets were used: MMP9, 5′-GCC TCA AGT GGG ACC ATC AT-3′ (forward) and 5′-CTC GCG GCA AGT CTT CAG A-3′ (reverse); MMP2, 5′-GCA GGG TGG TGG TCA TAG CTA-3′ (forward) and 5′-CAC GCT CTT GAG ACT TTG GTT CT-3′ (reverse); collagen I, 5′-GCC TTG GAG GAA ACT TTG CTT-3′ (forward) and 5′-GCA CGG AAA CTC CAG CTG AT-3′ (reverse); fibronectin, 5′-TAC CAA GGT CAA TCC ACA CCC C-3′ (forward) and 5′-CAG ATG GCA AAA GAA AGC AGA GG-3′ (reverse); and GAPDH, 5′-GAC GGC CGC ATC TTC TTG T-3′ (forward) and 5′-TCT CCA CTT TGC CAC TGC AA-3′ (reverse).

Retroviral Transduction—Cdc42$^{-/-}$ MEFs were reconstituted with retrovirus expressing HA-tagged Cdc42 with EGFP (MIEG3 vector). Wild-type Cdc42 (WT) or effector binding mutant of Cdc42, Cdc42-D38A, or Cdc42-I173A/L174A, was expressed at a similar level in cells as the endogenous Cdc42. These effector binding mutants contain a single point mutation in Cdc42, which inhibits binding to PAK or Par6/WASP (27). 48 h after viral transduction, cells were sorted by the GFP marker and used in subsequent functional assays.

RESULTS

Cdc42 Deficiency in MEFs Impairs Global ECM Remodeling Activity—To understand the role of Cdc42 in primary cell regulation, we used MEFs from Cdc42$^{loxP/loxP}$ homozygous mice generated previously (24) since direct Cdc42 knock-out mice (*i.e.* Cdc42$^{-/-}$) are embryonic lethal. Using an adenovirus expressing the Cre recombinase, we were able to efficiently delete the Cdc42 gene (supplemental Fig. 1*A*) and completely remove Cdc42 protein (supplemental Fig. 1*B*) without affecting cell viability within the time frame of the subsequent assays. This method allowed us to investigate the specific involvement of Cdc42 in primary cells without possible limitations imposed by using the traditional nonspecific bacterial toxins or dominant mutants to interfere with Cdc42 activity.

To assess the requirement of Cdc42 in global extracellular matrix remodeling, we employed the collagen contraction assay that manifests the ability of fibroblasts to contract the surrounding matrix. Cdc42$^{-/-}$ MEFs showed significantly decreased activity in collagen contraction over WT MEFs (Fig. 1*A*). While increasing cell numbers caused an increased contractility for both WT and Cdc42$^{-/-}$ cells, Cdc42$^{-/-}$ MEFs displayed reduced contraction activity *versus* WT MEFs proportional to the cell numbers (supplemental Fig. 2). These results indicate that Cdc42 is essential in the fibroblast-mediated collagen contraction and organization.

Cdc42 Deletion Causes Defective Cell Morphology in Three Dimensions—Because Cdc42 has been shown to regulate cell morphology in two dimensions, we hypothesized that it also affects cellular morphology in three dimensions, which may contribute to the ability of the cell to reorganize ECM. At the initial time of plating in collagen matrix, both WT and Cdc42$^{-/-}$ cells were spherical in appearance; however, over time, WT MEFs were able to extend protrusions, whereas the Cdc42$^{-/-}$ MEFs remained mostly spherical (Fig. 1*B*). At 6 h after plating (latest time point assessed from Fig. 1*A*), it is seen that WT MEFs have significantly more of these extensions than Cdc42$^{-/-}$ MEFs (Fig. 1*C*). Cytoskeleton staining revealed that in WT MEFs, microtubules were well aligned along these extensions, and F-actin was accumulated at the tips of the protrusions, whereas in Cdc42$^{-/-}$ MEFs, there were no analogous microtubule or actin structures (Fig. 2*A*). In two dimensions, Cdc42$^{-/-}$ MEFs exhibited irregular, elongated protrusions as opposed to WT MEFs that showed a spread-out morphology (supplemental Fig. 3*A*) (24). These data indicate that although Cdc42 is required for normal cell morphologies in both two-dimensional and three-dimensional conditions, it distinctly regulates cell protrusion in three dimensions.

Cdc42 Deletion Causes Defective Focal Complex Formation in Three Dimensions—The drastic defective morphology of Cdc42$^{-/-}$ MEFs prompted us to further examine the effect of Cdc42 loss on adhesion to the matrix in three dimensions because Cdc42 has previously been shown to play a role in cell adhesion to the underlying ECM in two dimensions (24). In three dimensions, WT MEFs had characteristic focal complexes at the end of cellular protrusions and along the length of the extended cell body, whereas Cdc42$^{-/-}$ MEFs showed no detectable focal complexes, even at small extensions as revealed

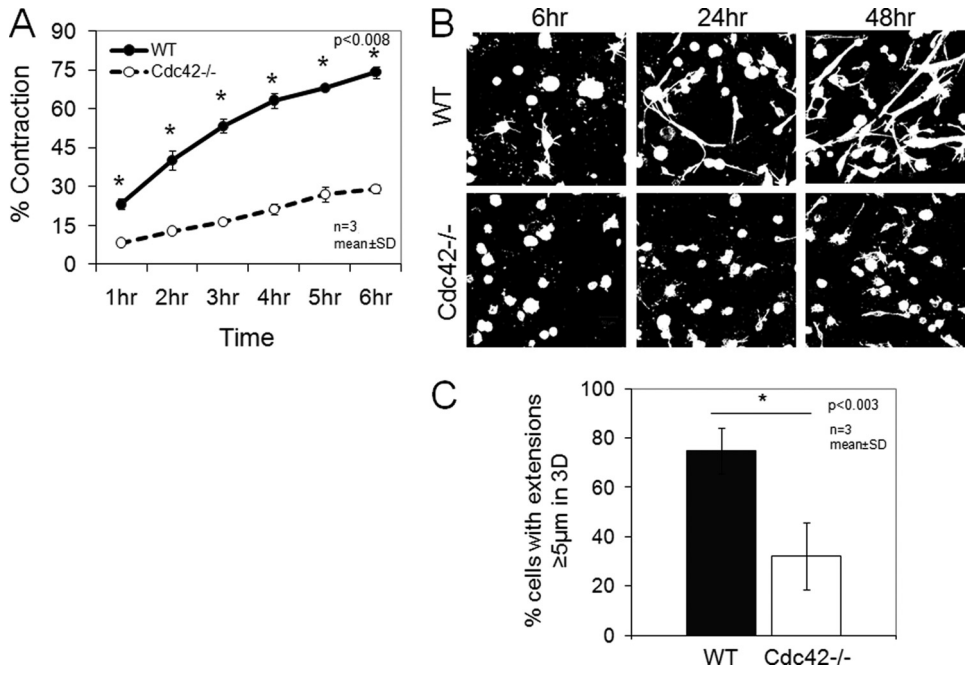

FIGURE 1. **Cdc42 deletion in MEFs decreases collagen contraction and prevents cell extensions in three dimensions.** WT or Cdc42$^{-/-}$ MEFs were plated in collagen1 at 150,000 cells/60 μl collagen gel. *A*, gel contraction increases over time, however with a significant reduction using Cdc42$^{-/-}$ MEFs. Mean ± S.D. ($n = 3$), $p < 0.01$. *B*, cells were fixed and immunostained with phalloidin to assess cellular morphology at 6, 24, and 48 h. WT MEF cells continue to elongate and spread, whereas Cdc42$^{-/-}$ MEFs remain compact. *C*, Cdc42$^{-/-}$ MEFs show a significant decrease in filipodia-like protrusions compared with WT MEFs in three dimensions at 6 h after plating. Images are representative of three independent experiments; mean ± S.D., $p < 0.005$. *3D*, three dimensions.

by phosphorylated paxillin immunostaining (Fig. 2*B*). In two dimensions, WT MEFs showed prominent focal complexes as seen by phosphorylated paxillin and vinculin immunostaining, whereas Cdc42$^{-/-}$ MEFs lacked these punctuated patches (supplemental Fig. 3*B*). These data indicate that Cdc42 is involved in cell adhesion in both three dimensions and two dimensions to the ECM.

Cdc42 Deletion Causes Defective Local ECM Remodeling by MEFs—The observations that loss of Cdc42 leads to a decrease in global ECM remodeling, a loss of normal MEF morphological maintenance, and a loss of focal complex components, led us to hypothesize that local ECM remodeling surrounding Cdc42$^{-/-}$ MEFs in three dimensions is also altered. To assess the effect of Cdc42 deficiency on the immediately surrounding matrix, we plated Cdc42$^{-/-}$ MEFs cells in three-dimensional collagen and visualized the cell bodies by rhodamine-phalloidin staining of F-actin and the collagen fibers around the cells by reflection microscopy. The ECM surrounding WT MEFs consisted of collagen fibrils that appear to extend from and align with the cellular protrusions (Fig. 3*A*). These aligned fibrils were not seen surrounding the Cdc42$^{-/-}$ MEFs, in which case the collagen alignment appeared random (Fig. 3*B*). A dark spherical region surrounding the WT MEF cell body suggests that these MEFs are able to degrade the immediate surrounding matrix, whereas Cdc42$^{-/-}$ MEFs lack this region. These data suggest that Cdc42 is involved in regulating the surrounding matrix and in matrix degradation.

Effect of Loss of Cdc42 on Extracellular Fibronectin Assembly—Fibronectin is a major constituent of the ECM produced by fibroblasts. *In vitro*, MEFs can make their own three-dimensional extracellular matrix composed of mainly fibronectin, which mimics *in vivo* mesenchymal matrices (26). To determine whether fibronectin matrix organization was altered by Cdc42 deficiency, we analyzed the MEF secreted ECM for fibronectin fiber structure and matrix thickness from WT and Cdc42$^{-/-}$ MEFs. WT MEFs produced an ECM with short, random fibronectin fiber alignment, whereas Cdc42$^{-/-}$ MEFs generated fibronectin fibers that were long and well aligned (Fig. 3*C*). The WT MEFs were also more proficient at producing fibronectin, as indicated by a thicker matrix compared with the Cdc42$^{-/-}$ MEFs (Fig. 3*D* and supplemental Fig. 4). Fibronectin and collagen synthesis and cellular fibronectin protein levels remained unchanged upon Cdc42 deletion (supplemental Fig. 5). These data indicate a role for Cdc42 in fibronectin ECM assembly surrounding the cells.

Effect of Loss of Cdc42 on Protease Processing—Proteases as well as constituents of the ECM secreted from cells play a role in the ECM organization. To examine whether Cdc42 may regulate protease processing, we plated the cells in three-dimensional collagen embedded with gelatin-fluorescence, which when cleaved by proteases becomes fluorescently activated. WT MEFs exhibited significantly higher protease activity than Cdc42$^{-/-}$ MEFs at 6, 24, and 48 h after plating (Fig. 4, *A* and *B*). Specific protease activities were detected around the periphery of WT MEFs, whereas mainly fluorescent signals inside cells were visible in Cdc42$^{-/-}$ MEFs (Fig. 4*C*). These data suggest that Cdc42 is involved in protease production and/or activation in ECM. To determine which proteases might be affected by the loss of Cdc42, we performed the collagen contraction assay and analyzed the surrounding media on a gel zymogram. The zymogram analysis revealed that WT MEF media contained both active and inactive forms of MMP9, whereas the media from Cdc42$^{-/-}$ MEFs contain only the inactive form of MMP9 (Fig. 4*D*). In contrast, MMP2 activity was not affected (supplemental Fig. 6*A*). In

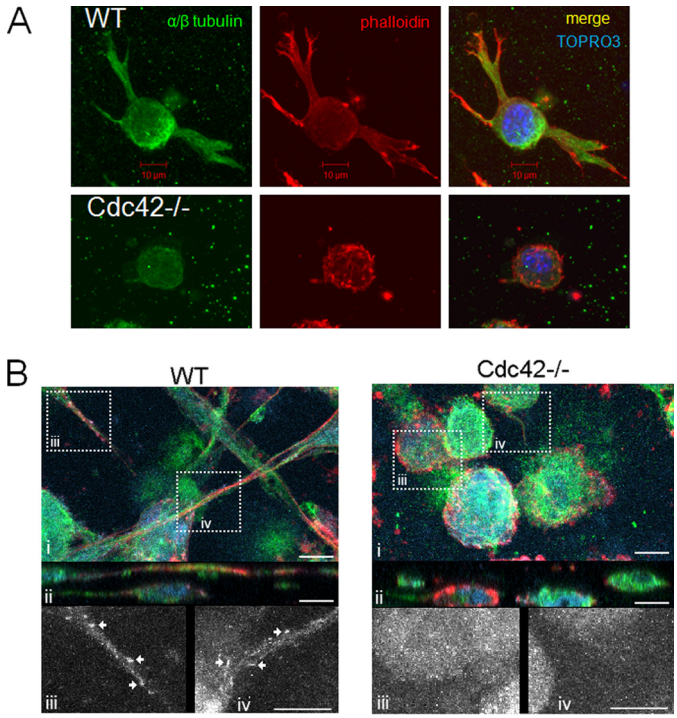

FIGURE 2. **Cytoskeletal organizations are disorganized and focal adhesions are reduced in Cdc42$^{-/-}$ MEFS in three dimensions.** WT or Cdc42$^{-/-}$ MEFs were plated in collagen 1 at 20,000 cells/collagen gel. *A*, cells were fixed and immunostained with anti-α/β tubulin (*green*) and phalloidin (*red*) at 6 h after plating. WT MEFs exhibit spread morphologies with aligned microtubules and actin-rich tips of extensions, whereas Cdc42$^{-/-}$ MEFs lack this organization. *B*, at 24 h after plating in three dimensions, WT MEFs reveal distinct punctate focal adhesion patterns, and Cdc42$^{-/-}$ MEFs have little to no focal adhesion complexes as shown with phospho-paxillin (*light blue*) immunostaining. *Arrows* in WT *inset* pictures (*panels iii* and *iv*) reveal focal adhesion complexes, whereas in the Cdc42$^{-/-}$ MEFs, the patterning was scarce. *Panel i* depicts a compressed confocal z-stack, whereas *panel ii* depicts a confocal z-stack across one XY plane. Colors in *B* represent actin in *red*, α/β tubulin in *green*, and paxillin in *light blue*.

addition, transcription of MMP9 (Fig. 4*E*), but not MMP2 (supplemental Fig. 6*B*), was found decreased in Cdc42$^{-/-}$ MEFs. These data strongly indicate that cellular Cdc42 is required for the expression and activation of MMP9.

To examine whether MMPs play a role in cellular matrix contractility, WT MEFs were treated with varying concentrations of a general MMP inhibitor, GM6001, and the collagen contractility assay was performed. This MMP inhibitor suppressed the gel contraction in a dose-dependent manner, from 80% to 75–62% at 5–20 μM of the inhibitor at the 5 h time point (supplemental Fig. 7). These results suggest that MMPs are partially involved in the contractility of matrix. Thus, Cdc42 regulates MMP9 expression and activation, which may contribute to the Cdc42-mediated ECM remodeling.

Cdc42 Deficiency Alters Focal Complex and Actin Organization Signal in Three Dimensions—Cdc42 controls a variety of downstream pathways to affect cell morphology, actin organization, and focal adhesion patterning that may be important in ECM remodeling. Signaling components important in these pathways include FAK, paxillin, WASP, PAK, cofilin, MLC, and integrins. To determine which downstream signaling molecules were affected by Cdc42 deletion in MEFs cultured in three dimensions, we analyzed phosphorylation states of these proteins by Western blotting. The phosphorylation activities of cytoskeletal organizing proteins PAK, WASP, and cofilin and focal adhesion proteins FAK and paxillin were decreased in the Cdc42$^{-/-}$ MEFs (Fig. 5, *A* and *B*). Integrin β3, a major subunit of intergins expressed in WT MEFs, was significantly decreased in Cdc42$^{-/-}$ MEFs as measured by flow cytometry (Fig. 5*C*). On the other hand, integrins β1 and α5 remained unchanged, although α4, αL, and αM subunits, which were expressed at low levels in MEFs, were also significantly altered upon Cdc42 deletion (Fig. 5*C*). These data indicate that loss of Cdc42 causes defects in downstream signaling pathways regulating actin organization and focal adhesion, which may contribute to the observed defect in ECM remodeling.

PAK but Not PAR6 or WASP Interaction Is Involved in ECM Thickness and Contractility Regulated by Cdc42—To determine which downstream signaling components of Cdc42 might be involved in ECM organization, we expressed the Cdc42 effector-binding mutants, Cdc42-D38A and Cdc42-I173A/L174A, which lack binding activity to the downstream effector PAK or PAR6/WASP (27), as well as WT Cdc42, in Cdc42$^{-/-}$ MEFs by retroviral transduction. PAK most notably regulates actin and microtubule dynamics, PAR6 is known to regulate microtubule polarity, whereas WASP is important for F-actin nucleation reaction. At a similar expression level to that of endogenous Cdc42 (Fig. 6*A*), the WT or PAR6/WASP-deficient, but not PAK-deficient, mutant of Cdc42 was able to rescue collagen contraction defect by Cdc42 knock-out (Fig. 6*B*), suggesting that PAK, but not PAR6/WASP, may be involved in collagen contraction. The PAK-binding defective mutant, but not the PAR6/WASP binding mutant, was able to rescue fibronectin matrix thickness (Fig. 6*C*). These data suggest that the PAK pathway is involved in Cdc42-mediated collagen contraction and native fibronectin organization by MEFs.

DISCUSSION

Cdc42 has previously been shown to regulate cell morphology, actin organization, and focal adhesion complexes *in vitro* and basement membrane organization and forebrain development *in vivo* (24, 28–30). There are several inherent limitations with these studies. First, they are performed in two-dimensional culture conditions, which hamper the ability to analyze cell-ECM interactions that occur in three dimensions. Second, *in vivo* studies show phenotypes that may have arisen due to inter-cellular interactions of neighboring cells and the downstream signaling pathways, and specific cellular functions involved are difficult to dissect. In the current work, we have genetically defined the role of Cdc42 in ECM remodeling in three dimensions and provide evidence that collected cell functions, including ECM adhesion, cytoskeleton organization, protease (MMP9) activation, and extracellular matrix component production and organization, may be involved in generating the ECM environment (Fig. 5*D*). Furthermore, we implicate the immediate downstream signaling effector PAK as a candidate pathway through which Cdc42 exerts these functions.

The fibroblast contraction of a collagen gel is a commonly used model system to evaluate cell-ECM interactions in three-dimensional environments. The simplicity of the contraction assay allows for the analysis of cell-ECM interactions without

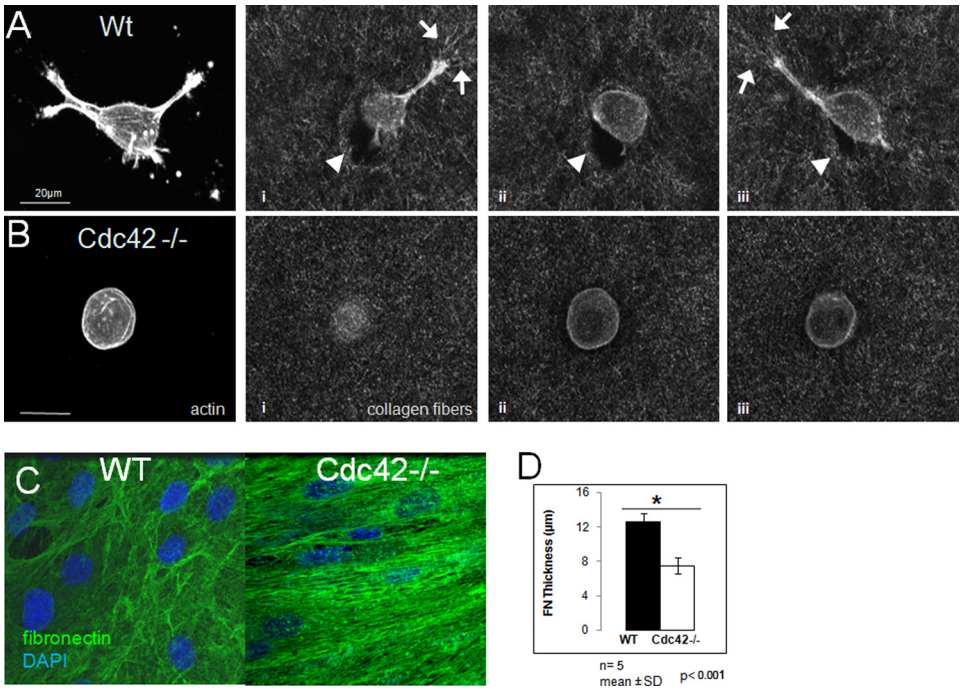

FIGURE 3. **Cdc42 is necessary for local exogenous collagen remodeling and native fibronectin organization and alignment in three dimensions.** WT or Cdc42$^{-/-}$ MEFs were plated in collagen 1 at 20,000 cells/60 μl 50% collagen gel (*A* and *B*) or allowed to produce their own matrix (*C*). At 6 h after plating in three dimensions, WT MEFs appear to grab the matrix (*A*, *panels i–iii*) and pull on the collagen fibrils (*arrows*). *Arrowheads* indicate a hole in the matrix near WT cell. Cdc42$^{-/-}$ MEFs remain compact (*B*, *panels i–iii*). *Panels i–iii* depict representative z-stacks (at ~4 μm intervals) and show collagen matrix fibril alignment measured by reflection microscopy. The images on the *far left* are the compressed z-stacks with phalloidin immunostaining of F-actin. *C* and *D*, Cdc42$^{-/-}$ MEFs were encouraged to produce a three-dimensional FN matrix with the addition of ascorbic acid (50 μg/ml) every other day, resulting in a thinner and more aligned fibronectin matrix than WT MEFs at 8 days post-plating. $n = 5$, mean ± S.D., $p < 0.001$.

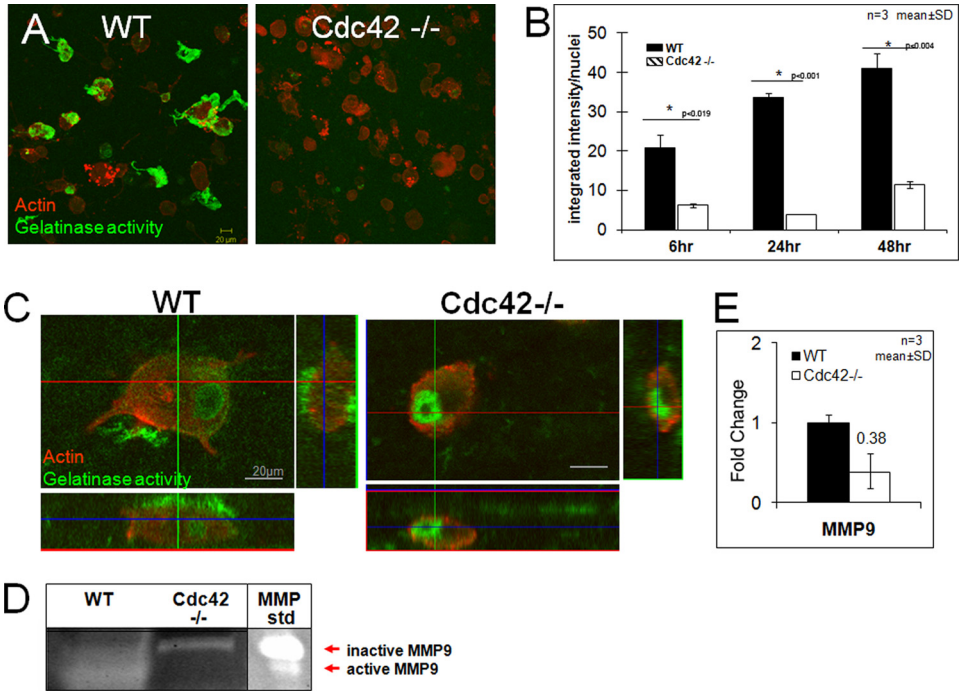

FIGURE 4. **Cdc42 is necessary for MMP9 activation and expression in three dimensions.** To detect extracellular matrix changes due to gelatinases, WT or Cdc42$^{-/-}$ MEFs were plated in collagen 1 at 20,000 cells/collagen gel with fluorescent gelatin (*green*) mixed in the collagen gel, and cleavage of the gelatin was detected by fluorescence. *A* and *B*, gelatinase activity is significantly higher in the WT than in the Cdc42$^{-/-}$ MEFs ($n = 3$, mean ± S.D., $p < 0.01$). *A* is imaged at 24 h after plating. *C*, active gelatinase activity is shown along the outside periphery of WT MEFs but remains inside Cdc42$^{-/-}$ MEFs at 6 h after plating. Z-stacks along the *green* and *red line* planes are also shown. Cdc42$^{-/-}$ MEFs show a reduction of MMP9 activation (*D*) as shown by zymography from WT and Cdc42$^{-/-}$ MEF media at 6 h post plating (*D*) and MMP9 transcripts as shown by RT-PCR (*E*) at 24 h post plating ($n = 3$, mean ± S.D.). *std*, standard.

compounding factors seen *in vivo*. In collagen matrices, normal fibroblasts extend processes over time to contract the matrix. Addition of lysophosphatidic acid or PDGF was shown to stimulate RhoA and Rac1, respectively, and was found to increase matrix contraction, which was inhibited by pertussis toxin (21, 31). In two dimensions, Cdc42 has been shown to be down-

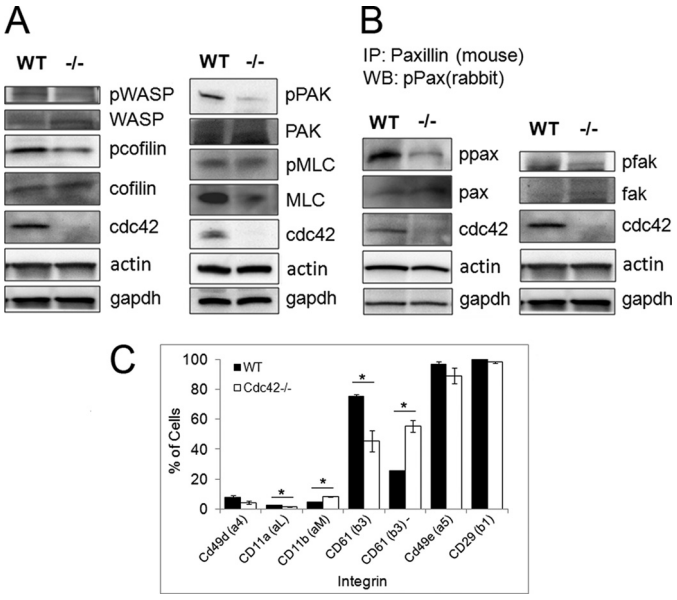

FIGURE 5. **Cdc42 regulates the activation states of WASP, cofilin, PAK, paxillin, and FAK and expression of integrins in three dimensions.** WT or Cdc42$^{-/-}$ MEFs plated in three-dimensional collagen 1 after 6 h of plating were analyzed using Western blotting. The phosphorylation of actin cytoskeletal modulators WASP, cofilin, and PAK (*A*) and focal adhesion components paxillin (*pax*) and FAK (*B*) are decreased upon Cdc42 deletion in MEFs. Phosphorylation status of MLC appears to be level; however, total protein levels are decreased upon Cdc42 deletion. *B*, actin and GAPDH were run in total cell lysates. *C*, flow cytometry analysis of integrin subunits, β1, β3, α4, αL, αM, and α5 in WT and Cdc42$^{-/-}$ MEFS ($n = 3$, mean $\pm$ S.D.). *WB*, Western blot.

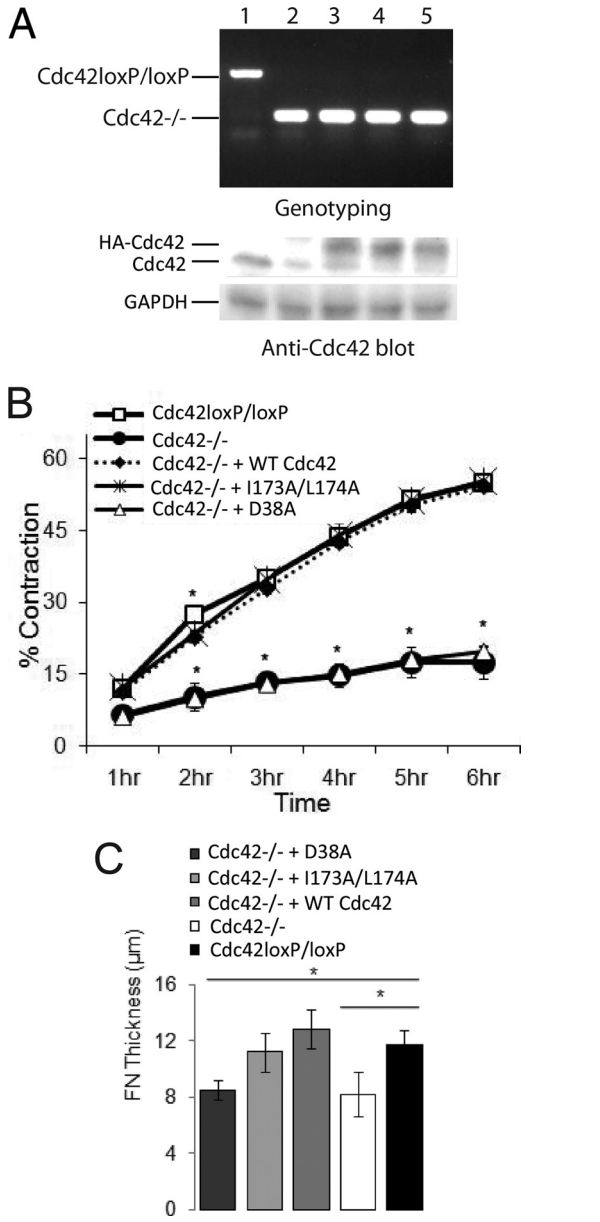

FIGURE 6. **Rescue of ECM remodeling by Cdc42 mutant reconstitution.** *A*, genomic DNA genotyping and Western blot confirm endogenous Cdc42 deletion and WT or mutant Cdc42 protein reconstitution in Cdc42$^{loxP/loxP}$ MEFs with or without Cre treatment. *Lane 1*, Cdc42$^{loxP/loxP}$ cells; *lane 2*, Cdc42$^{loxP/loxP+cre}$; *lane 3*, Cdc42$^{loxP/loxP+cre+WT\ HA\text{-}Cdc42}$; *lane 4*, Cdc42$^{loxP/loxP+cre+HA\text{-}D38A}$; *lane 5*, Cdc42$^{loxP/loxP+cre+HA\text{-}I173A/L174A}$. *B*, the collagen matrix contraction assays were carried out with Cdc42 effector binding mutant MEFs ($n = 3$, mean $\pm$ S.D., and $p < 0.004$ for Cdc42$^{-/-}$ and PAK mutant compared with WT for the 2–6 h time points and for Cdc42$^{-/-}$ and PAR6 mutant compared with WT for the 2-h time point). *C*, the thickness of fibronectin matrix produced by Cdc42 WT or mutant reconstituted MEFs was measured by confocal z-stack at 9 days after plating of the cells ($n = 7$, mean $\pm$ S.D., $p < 0.001$).

stream of LPA stimulation and inhibited by pertussis toxin (32). Our studies using Cdc42$^{-/-}$ MEFs show that matrix contraction is significantly reduced, demonstrating that Cdc42 is essential for efficient matrix contraction (Fig. 1 and supplemental Fig. 2). This functional outcome in three dimensions is closely related to the observed cytoskeleton and morphological changes and to the signaling decreases of phospho-PAK, -WASP, and -cofilin, as previous studies have found that PAK and cofilin inhibition decreases matrix contraction (20).

The general paradigm of matrix contraction is thought to be through cell-matrix interactions, which generate cellular tractional force through the cell migratory machinery and cytoskeletal dynamics, and mechanical loading (2, 33). Cdc42 is known to regulate cell migration in two dimensions by modulating cell morphology and focal adhesion. We have previously shown that conditional Cdc42$^{-/-}$ MEFs have irregular shaped morphologies with contracting cell bodies and reduced focal adhesion complexes (24), whereas others found Cdc42 knock-out ES cells to be smaller and exhibit round morphologies (28). WT MEFs in three dimensions exhibit extended morphologies with actin-rich extensions and phospho-paxillin containing focal adhesion complexes, whereas loss of Cdc42 results in a round morphology with a disorganized cytoskeleton (Fig. 1, *B* and *C*, and Fig. 2) and a lack of detectable focal adhesion complexes (Fig. 2*B*). Furthermore, the phosphorylation of focal adhesion proteins, FAK and paxillin, was decreased in Cdc42$^{-/-}$ MEFs (Fig. 5*B*) as the integrin β3 expression, which is known to bind to fibronectin among other substrates (Fig. 5*C*). Consistent with previous findings in two dimensions, these data suggest that Cdc42 is necessary for regulating cell morphology and focal complex formation in three dimensions. Because efficient cell-ECM binding is necessary for effective matrix contraction (34, 35), the lack of focal complexes in Cdc42$^{-/-}$ MEFs likely contributes to the decreased ability to contract the matrix. Although these cells have altered surface integrin expressions, they still retain partial activity in contracting the matrix, which is likely due to an amoeboid-like migration reminiscent of cancer cell migration when MMPs are removed (36). The reduc-

tion in MMPs may affect proper processing of the fibronectin fibrils, which results in decreased matrix contraction and a differential cellular phenotype (*i.e.* round) in three dimensions than in two dimensions. This effect on the inside-out cell-matrix interaction may be related to the activities of actin organization proteins such as PAK, cofilin, and WASP, which were decreased in the Cdc42$^{-/-}$ MEFs (Fig. 5*A*).

ECM contraction can also be a result of the ability of the cell to locally remodel the ECM. In three-dimensional collagen gels, ECM fiber alignment surrounding the fibroblasts is rearranged (5, 37). WT MEFs show local collagen fibril alignment organized along the long axis of the extension of the cells, whereas Cdc42$^{-/-}$ MEFs lack collagen fibril reorganization capability (Fig. 3*A*). This finding fits well with the observed defects in focal adhesion complexes and cytoskeletal organization of the knock-out cells because both are required for the cellular traction and mechanical force, which are, in turn, required for the fibril alignment force. Other major regulators and linkers of cellular force and ECM remodeling include integrins. With the observation that focal complex is disrupted in Cdc42-deficient fibroblasts, we expect that integrin activities are also defective downstream of Cdc42 and contribute to the altered ECM organization. In addition to the defective collagen fibrils, we found that MEFs deficient in Cdc42 are defective in three-dimensional fibronectin deposition but not synthesis, particularly in altering fibronectin thickness and alignment structure (Fig. 3, *C–E*). Whether such altered ECM can promote or suppress tumor cell migration, invasion, or proliferation will be interesting to test. A recent study evaluating native fibronectin matrix production shows that tumor-associated fibroblasts generate fibronectin with similar morphology and aligned fibronectin pattern (38) as the Cdc42$^{-/-}$ MEFs, raising the possibility that fibronectin organization around the tumors may be modulated by a reduced Cdc42 activity in the tumor-associated fibroblasts.

MMPs were thought previously to be involved in regulating fibroblast-mediated ECM contraction through ECM cleavage and degradation and may do so by interfering with tractional forces and migration and competing with cell-matrix proteins (8, 13, 14). Because Cdc42 has previously been shown to regulate two-dimensional cell adhesion and migration, as well as the activation and secretion of MMPs (15, 24, 39), we wanted to further evaluate the role of Cdc42 on MMP activity in three dimensions. In our system, MMP9 activity is decreased upon Cdc42 deletion and mostly remains inside the Cdc42$^{-/-}$ cell (Fig. 4, *A–C*). The transcription and activity levels of MMP9 are also decreased in Cdc42$^{-/-}$ media, whereas MMP2 transcription and activity levels are unchanged (Fig. 4, *D* and *E*, and supplemental Fig. 6). Consistently, ERK activity, which may affect MMP2 transcription, is not affected in Cdc42$^{-/-}$ MEFs (supplemental Fig. 8). Because MMPs are necessary for efficient matrix remodeling and contractivity, it is likely that the altered MMP9 activity due to Cdc42 deletion is contributing to the phenotype of inefficient three-dimensional ECM remodeling. Future studies are warranted to determine the role of Cdc42 in three-dimensional ECM remodeling, particularly in the context of recent finding from Friedl's group (40, 41), which elegantly shows that the nature of the collagen gel and pore size determines whether ameboid movement is MMP dependent or independent, and work from Yamada *et al.* (42, 43), which implicates cell adhesion structures and ECM fibrils in the formation of three-dimensional matrices.

We have made an attempt to delineate the effector signaling events involved in this Cdc42 function. Among the known effector targets, PAK specifically has been shown to play a role in LPA- and PDGF-stimulated ECM contraction. In agreement with these, we show that PAK activity is decreased in Cdc42$^{-/-}$ cells and mutant of Cdc42 deficient in binding to PAK could not rescue the contractility activity, suggesting that in our system PAK plays a role in mediating Cdc42 signaling to ECM remodeling. Additionally, microtubule dynamics have been shown to play a role in fibroblast morphology in three dimensions (44). Because Cdc42 is known to regulate microtubule dynamics and polarity (22), the rounded morphology in Cdc42$^{-/-}$ MEFs may also be due to altered microtubule organization. However, addition of PAR6/WASP binding-deficient Cdc42 mutant to Cdc42$^{-/-}$ MEFs was able to rescue collagen contraction and fibronectin remodeling, indicating that Cdc42-regulated microtubule polarity may not be involved in ECM remodeling. It remains to be seen how other signaling pathways controlled by Cdc42, *e.g.* IQGAP, N-WASP, and MCRK, may contribute to different aspects of the global ECM remodeling.

In conclusion, our study identifies a novel function for Cdc42 in regulating ECM structure in three dimensions. How Cdc42 would exert such a role in physiologically and pathologically relevant conditions involving dynamic interactions of cells with ECM such as wound healing, embryonic development, or tumor progression is an important topic that requires future experimentations. Altogether, Cdc42 and its signaling pathways play critical roles in cell morphogenesis and matrix remodeling, manipulation of which may benefit diseases including cancer and regenerative medicine such as tissue engineering.

Acknowledgments—We thank James F. Johnson, Clara B. Blair, and Kaari Lynch for technical support and Dr. Shirin Akter for providing the adenovirus containing Cre recombinase.

REFERENCES

1. Beacham, D. A., and Cukierman, E. (2005) *Semin. Cancer Biol.* **15,** 329–341
2. Grinnell, F. (2003) *Trends Cell Biol.* **13,** 264–269
3. Cukierman, E., Pankov, R., and Yamada, K. M. (2002) *Curr. Opin. Cell Biol.* **14,** 633–639
4. Cukierman, E., Pankov, R., Stevens, D. R., and Yamada, K. M. (2001) *Science* **294,** 1708–1712
5. Lakshman, N., Kim, A., Bayless, K. J., Davis, G. E., and Petroll, W. M. (2007) *Cell Motil. Cytoskeleton* **64,** 434–445
6. Ishii, I., Tomizawa, A., Kawachi, H., Suzuki, T., Kotani, A., Koshushi, I., Itoh, H., Morisaki, N., Bujo, H., Saito, Y., Ohmori, S., and Kitada, M. (2001) *Atherosclerosis* **158,** 377–384
7. Yamada, K. M., and Cukierman, E. (2007) *Cell* **130,** 601–610
8. Phillips, J. A., Vacanti, C. A., and Bonassar, L. J. (2003) *Biochem. Biophys. Res. Commun.* **312,** 725–732
9. Meshel, A. S., Wei, Q., Adelstein, R. S., and Sheetz, M. P. (2005) *Nat. Cell Biol.* **7,** 157–164
10. Petroll, W. M., and Ma, L. (2003) *Cell Motil. Cytoskeleton* **55,** 254–264
11. Katsumi, A., Orr, A. W., Tzima, E., and Schwartz, M. A. (2004) *J. Biol. Chem.* **279,** 12001–12004

12. Bershadsky, A. D., Balaban, N. Q., and Geiger, B. (2003) *Annu. Rev. Cell Dev. Biol.* **19,** 677–695
13. Daniels, J. T., Cambrey, A. D., Occleston, N. L., Garrett, Q., Tarnuzzer, R. W., Schultz, G. S., and Khaw, P. T. (2003) *Invest. Ophthalmol. Vis. Sci.* **44,** 1104–1110
14. Defawe, O. D., Kenagy, R. D., Choi, C., Wan, S. Y., Deroanne, C., Nusgens, B., Sakalihasan, N., Colige, A., and Clowes, A. W. (2005) *Cardiovasc. Res.* **66,** 402–409
15. Deroanne, C. F., Hamelryckx, D., Ho, T. T., Lambert, C. A., Catroux, P., Lapière, C. M., and Nusgens, B. V. (2005) *J. Cell Sci.* **118,** 1173–1183
16. Nobes, C. D., and Hall, A. (1995) *Cell* **81,** 53–62
17. Zhuge, Y., and Xu, J. (2001) *J. Biol. Chem.* **276,** 16248–16256
18. Turchi, L., Chassot, A. A., Bourget, I., Baldescchi, C., Ortonne, J. P., Meneguzzi, G., Lemichez, E., and Ponzio, G. (2003) *J. Invest. Dermatol.* **121,** 1291–1300
19. Heasman, S. J., and Ridley, A. J. (2008) *Nat. Rev. Mol. Cell Biol.* **9,** 690–701
20. Rhee, S., and Grinnell, F. (2006) *J. Cell Biol.* **172,** 423–432
21. Grinnell, F., Ho, C. H., Tamariz, E., Lee, D. J., and Skuta, G. (2003) *Mol. Biol. Cell* **14,** 384–395
22. Melendez, J., Grogg, M., and Zheng, Y. (2011) *J. Biol. Chem.* **286,** 2375–2381
23. Wang, L., and Zheng, Y. (2007) *Trends Cell Biol.* **17,** 58–64
24. Yang, L., Wang, L., and Zheng, Y. (2006) *Mol. Biol. Cell* **17,** 4675–4685
25. Guo, F., Debidda, M., Yang, L., Williams, D. A., and Zheng, Y. (2006) *J. Biol. Chem.* **281,** 18652–18659
26. Beacham, D. A., Amatangelo, M. D., and Cukierman, E. (2007) *Curr. Protoc. Cell Biol.* **10,** 9–15
27. Guo, F., Hildeman, D., Tripathi, P., Velu, C. S., Grimes, H. L., and Zheng, Y. (2010) *Proc. Natl. Acad. Sci. U.S.A.* **107,** 18505–18510
28. Chen, F., Ma, L., Parrini, M. C., Mao, X., Lopez, M., Wu, C., Marks, P. W., Davidson, L., Kwiatkowski, D. J., Kirchhausen, T., Orkin, S. H., Rosen, F. S., Mayer, B. J., Kirschner, M. W., and Alt, F. W. (2000) *Curr. Biol.* **10,** 758–765
29. Wu, X., Quondamatteo, F., and Brakebusch, C. (2006) *Matrix Biol.* **25,** 466–474
30. Chen, L., Liao, G., Yang, L., Campbell, K., Nakafuku, M., Kuan, C. Y., and Zheng, Y. (2006) *Proc. Natl. Acad. Sci. U.S.A.* **103,** 16520–16525
31. Grinnell, F., Ho, C. H., Lin, Y. C., and Skuta, G. (1999) *J. Biol. Chem.* **274,** 918–923
32. Ueda, H., Morishita, R., Yamauchi, J., Itoh, H., Kato, K., and Asano, T. (2001) *J. Biol. Chem.* **276,** 6846–6852
33. Dahlmann-Noor, A. H., Martin-Martin, B., Eastwood, M., Khaw, P. T., and Bailly, M. (2007) *Exp. Cell Res.* **313,** 4158–4169
34. Gullberg, D., Tingström, A., Thuresson, A. C., Olsson, L., Terracio, L., Borg, T. K., and Rubin, K. (1990) *Exp. Cell Res.* **186,** 264–272
35. Klein, C. E., Dressel, D., Steinmayer, T., Mauch, C., Eckes, B., Krieg, T., Bankert, R. B., and Weber, L. (1991) *J. Cell Biol.* **115,** 1427–1436
36. Wolf, K., Mazo, I., Leung, H., Engelke, K., von Andrian, U. H., Deryugina, E. I., Strongin, A. Y., Bröcker, E. B., and Friedl, P. (2003) *J. Cell Biol.* **160,** 267–277
37. Kim, A., Lakshman, N., and Petroll, W. M. (2006) *Exp. Cell Res.* **312,** 3683–3692
38. Quiros, R. M., Valianou, M., Kwon, Y., Brown, K. M., Godwin, A. K., and Cukierman, E. (2008) *Gynecol. Oncol.* **110,** 99–109
39. Ispanovic, E., Serio, D., and Haas, T. L. (2008) *Am. J. Physiol. Cell Physiol.* **295,** C600–610
40. Ilina, O Bakker, G. J., Vasaturo, A, Hofmann, R. M., and Friedl, P. (2011) *Phys. Biol.* **8,** 015010
41. Wolf, K, Alexander, S, Schacht, V, Coussens, L. M, von Andrian, U. H, van Rheenen, J, Deryugina, and E, Friedl, P. (2009) *Semin. Cell Dev. Biol.* **20,** 931–941
42. Hakkinen, K. M., Harunaga, J. S., Doyle, A. D., and Yamada, K. M. (2011) *Tissue Engineering Part A* **17,** 713–724
43. Harunaga, J. S, and Yamada, K. M. (2011) *Matrix Biol.* [Epub ahead of print]
44. Rhee, S., Jiang, H., Ho, C. H., and Grinnell, F. (2007) *Proc. Natl. Acad. Sci. U.S.A.* **104,** 5425–5430